

## STUDY OF THE $e^+e^- \rightarrow Z e^+e^-$ PROCESS AT LEP

R. VASQUEZ

*Purdue University, Department of Physics  
525 Northwestern Avenue, West Lafayette, IN 47907-2036 USA,  
E-mail: ricardo@physics.purdue.edu*

The cross section of the process  $e^+e^- \rightarrow Ze^+e^-$  is measured with  $0.7\text{fb}^{-1}$  of data collected with the L3 detector at LEP. Decays of the Z boson into quarks and muons are considered at centre-of-mass energies ranging from 183 GeV up to 209 GeV. The measurements are found to agree with Standard Model predictions.

### 1. Introduction

The study of gauge boson production in  $e^+e^-$  collisions constitutes one of the main subjects of the scientific program carried out at LEP. Above the Z resonance “single” weak gauge bosons can also be produced via  $t$ -channel processes<sup>1,2</sup>. A common feature of this single boson production is the emission of a virtual photon off the incoming electron or positron. This electron or positron remains in turn almost unscattered at very low polar angles and hence not detected. Figure 1 presents two Feynman diagrams for the single

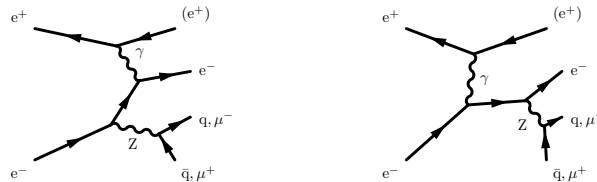


Figure 1. Main diagrams contributing to the “single Z” production.

Z production, followed by the decay of the Z into a quark–antiquark or a muon–antimuon pair. The signal definition applied in this study requires the final state fermions to satisfy the kinematical cuts

$$\begin{aligned}
 m_{\bar{f}f} &> 60 \text{ GeV}, \quad \theta_{\text{unscattered}} < 12^\circ, \quad 60^\circ < \theta_{\text{scattered}} < 168^\circ, \\
 E_{\text{scattered}} &> 3.0 \text{ GeV},
 \end{aligned}
 \tag{1}$$

where  $m_{f\bar{f}}$  refers to the invariant mass of the produced quark–antiquark or muon–antimuon pair,  $\theta_{unscattered}$  is the polar angle at which the electron<sup>a</sup> closest to the beam line is emitted,  $\theta_{scattered}$  and  $E_{scattered}$  are respectively the polar angle with respect to its incoming direction and the energy of the electron scattered at the largest polar angle.

## 2. Data and Monte Carlo samples

This analysis is based on  $675.5 \text{ pb}^{-1}$  of integrated luminosity collected at  $\sqrt{s} = 182.7 - 209.0 \text{ GeV}$  with the L3 detector<sup>3</sup>. For the investigation of the  $e^+e^- \rightarrow Ze^+e^- \rightarrow q\bar{q}e^+e^-$  channel, this sample is divided into eight different energy bins whose corresponding average  $\sqrt{s}$  values and integrated luminosities are reported in Table 1. The signal process is mod-

Table 1. The average centre-of-mass energies and the corresponding integrated luminosities of the data sample used in this study.

$\sqrt{s} [\text{GeV}]$	182.7	188.6	191.6	195.5	199.5	201.7	204.9	206.6
$\mathcal{L} [\text{pb}^{-1}]$	55.1	176.0	29.4	83.0	80.8	36.7	76.6	137.9

elled with the WPHACT Monte Carlo program<sup>4</sup>. Events are generated in a phase space broader than the one defined by the criteria (1). Those events who do not satisfy these criteria are considered as background. The GRC4F<sup>5</sup> event generator is used for systematic checks. The  $e^+e^- \rightarrow q\bar{q}(\gamma)$ ,  $e^+e^- \rightarrow \mu^+\mu^-(\gamma)$  and  $e^+e^- \rightarrow \tau^-\tau^+(\gamma)$  processes are simulated with the KK2f<sup>6</sup> Monte Carlo generator, the  $e^+e^- \rightarrow ZZ$  process with PYTHIA<sup>7</sup>, and the  $e^+e^- \rightarrow W^+W^-$  process, with the exception of the  $q\bar{q}'e\nu$  final state, with KORALW<sup>8</sup>. EXCALIBUR<sup>9</sup> is used to simulate the  $q\bar{q}'e\nu$  and other four–fermion final states. Hadron and lepton production in two–photon interactions are modelled with PHOJET<sup>10</sup> and DIAG36<sup>11</sup>, respectively. The generated events are passed through the L3 detector simulation program<sup>12</sup>.

## 3. Event selection

### 3.1. $e^+e^- \rightarrow Ze^+e^- \rightarrow q\bar{q}e^+e^-$ channel

The selection of events in the  $e^+e^- \rightarrow Ze^+e^- \rightarrow q\bar{q}e^+e^-$  channel proceeds from high multiplicity events with at least one electron identified in the BGO electromagnetic calorimeter and in the central tracker with an energy

<sup>a</sup>The word “electron” is used for both electrons and positrons.

above 3 GeV. The signal topology is enforced requiring events with a reconstructed invariant mass of the hadronic system, stemming from a  $Z$  boson, between 50 and 130 GeV, a visible energy of at least  $0.40\sqrt{s}$  and a missing momentum, due to the undetected electron, of at least  $0.24\sqrt{s}$ . Due to the particular signature of an electron undetected at low angle and the other scattered in the detector, two powerful kinematic variables can be considered: the product of the charge,  $q$ , of the detected electron and the cosine of its polar angle measured with respect to the direction of the incoming electron,  $\cos\theta$ , and the product of  $q$  and the polar angle of the direction of the missing momentum,  $\cos\phi$ . Two selection criteria are applied:

$$q \times \cos\theta > -0.5 \text{ and } q \times \cos\phi > 0.94,$$

Distributions of these variables are presented in Fig. 2.

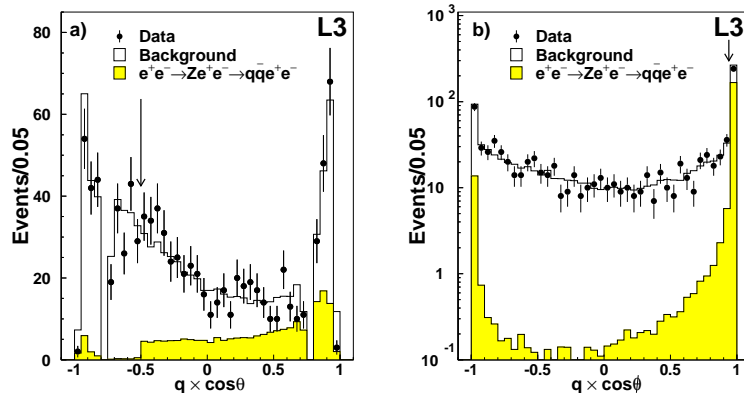


Figure 2. Distributions for data, signal and background Monte Carlo of the product of the charge of the detected electron and a) the cosine of its polar angle and b) the cosine of the polar angle of the missing momentum. The arrows show the position of the applied cuts. All other selection criteria but those on these two variables are applied. Signal events around  $-1$  correspond to charge confusion in the central tracker. The sharp edge of the signal distribution in a) at  $-0.5$  follows from the signal definition criterion  $\theta_{scattered} > 60^\circ$ ; moreover, the depletion around  $\pm 0.7$  in data and Monte Carlo is due to the absence of the BGO calorimeter in this angular region.

### 3.2. $e^+e^- \rightarrow Ze^+e^- \rightarrow \mu^+\mu^-e^+e^-$ channel

Candidates for the  $e^+e^- \rightarrow Ze^+e^- \rightarrow \mu^+\mu^-e^+e^-$  process are selected by first requiring low multiplicity events with three tracks in the cen-

tral tracker, corresponding to one electron with energy above 3 GeV and two muons, reconstructed in the muon spectrometer with momenta above 18 GeV. A kinematic fit is then applied which requires momentum conservation in the plane transverse to the beam axis. The reconstructed invariant mass of the two muons should lie between 55 and 145 GeV. Finally, three additional selection criteria are applied:

$$-0.50 < q \times \cos \theta < 0.93, \quad q \times \cos \theta > 0.50 \quad \text{and} \quad q \times \cos \theta_Z < 0.40,$$

where  $\cos \theta_Z$  is the polar angle of the Z boson as reconstructed from the two muons. These criteria select 9 data events and  $6.6 \pm 0.1$  expected events from signal Monte Carlo with an efficiency of 22%. Background expectations amount to  $1.5 \pm 0.1$  events, coming in equal parts from muon-pair production in two-photon interactions, the  $e^+e^- \rightarrow \mu^+\mu^-(\gamma)$  process, and  $e^+e^- \rightarrow \mu^+\mu^-e^+e^-$  events generated with WPHACT that do not pass the signal definition criteria.

#### 4. Results

Figure 3a presents the distribution of the invariant mass of the hadronic system after applying all selection criteria of the  $e^+e^- \rightarrow Ze^+e^- \rightarrow q\bar{q}e^+e^-$  channel. A large signal peaking around the mass of the Z boson is observed. The single Z cross section at each value of  $\sqrt{s}$  is determined from a maximum-likelihood fit to the distribution of this variable. Results are given in Fig. 4 and show a good agreement with the WPHACT Monte Carlo. This agreement is quantified by extracting the ratio  $R$  between the measured cross sections  $\sigma^{\text{Measured}}$  and the WPHACT predictions  $\sigma^{\text{Expected}}$ :

$$R = \frac{\sigma^{\text{Measured}}}{\sigma^{\text{Expected}}} = 0.88 \pm 0.08 \pm 0.06,$$

where the first uncertainty is statistical and the second systematic.

The invariant mass of muon pairs from the  $e^+e^- \rightarrow Ze^+e^- \rightarrow \mu^+\mu^-e^+e^-$  selected events is shown in Fig. 3b. The cross section of this process is determined with a fit to the invariant mass distribution, over the full data sample, as:

$$\sigma(e^+e^- \rightarrow Ze^+e^- \rightarrow \mu^+\mu^-e^+e^-) = 0.043_{-0.013}^{+0.013} \pm 0.003 \text{ pb},$$

where the first uncertainty is statistical and the second systematic. This measurement agrees with the Standard Model prediction of 0.044 pb calculated with the WPHACT program as the luminosity weighted average cross section over the different centre-of-mass energies.

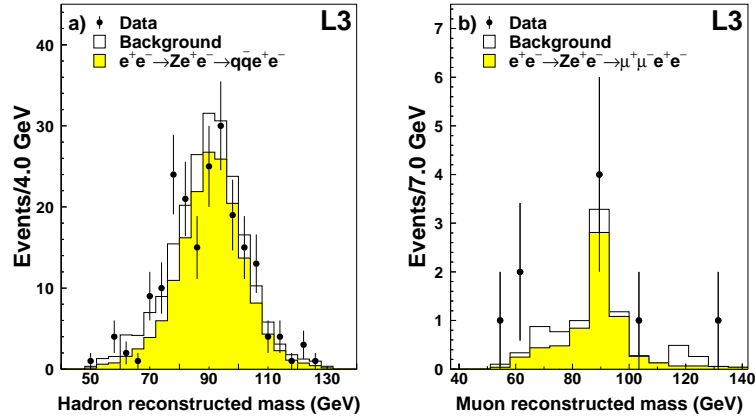


Figure 3. Distribution of the reconstructed invariant mass of a) the hadron system and b) the muon system for data, signal, and background Monte Carlo events.

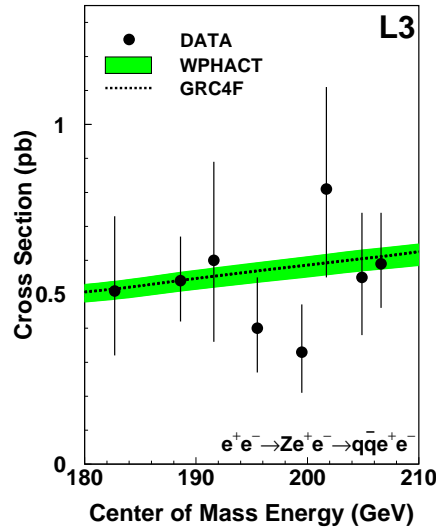


Figure 4. Measurements of the cross section of the  $e^+e^- \rightarrow Ze^+e^- \rightarrow q\bar{q}e^+e^-$  process as a function of the centre-of-mass energy. The WPHACT predictions are assigned an uncertainty of 5%. As reference, a line indicates the GRC4F expectations.

Several possible sources of systematic uncertainty and their effects on the measured cross sections are considered <sup>1</sup>. Uncertainties related to the energy scales of the calorimeters have the largest impact on the measurements: 2.3% and 6.3% on the  $q\bar{q}e^+e^-$  and  $\mu^+\mu^-e^+e^-$  cross sections, respectively.

In conclusion, the process  $e^+e^- \rightarrow Ze^+e^-$  has been observed at LEP for decays of the Z boson into both hadrons and muons. The measured cross sections have been compared with the Standard Model predictions, and were found in agreement with an experimental accuracy of about 10% for decays of the Z boson into hadrons.

## References

1. L3 Collab., M. Acciarri *et al.*, preprint hep-ex/0303041, and references therein
2. DELPHI Collab., P. Abreu *et al.*, *Phys. Lett.***B 515** (2001) 238; OPAL Collab., G. Abbiendi *et al.*, *Phys. Lett.* **B 438** (1998) 391; OPAL Collab., G. Abbiendi *et al.*, *Eur. Phys. J.* **C 24** (2002) 1
3. L3 Collab., B. Adeva *et al.*, *Nucl. Instr. Meth.* **A 289** (1990) 35; O. Adriani *et al.*, *Phys. Reports* **236** (1993) 1; M. Chemarin *et al.*, *Nucl. Instr. Meth.***A 349** (1994) 345; M. Acciarri *et al.*, *Nucl. Instr. Meth.***A 351** (1994) 300; G. Basti *et al.*, *Nucl. Instr. Meth.***A 374** (1996) 293; I.C. Brock *et al.*, *Nucl. Instr. Meth.***A 381** (1996) 236; A. Adam *et al.*, *Nucl. Instr. Meth.***A 383** (1996) 342
4. WPHACT version 2.1; E. Accomando and A. Ballestrero, *Comp. Phys. Comm.* **99** (1997) 270; E. Accomando, A. Ballestrero and E. Maina, preprint hep-ph/0204052 (2002)
5. GRC4F version 2.1; J. Fujimoto *et al.*, *Comp. Phys. Comm.* **100** (1997) 128
6. KK2f version 4.13; S. Jadach, B.F.L. Ward and Z. Was, *Comp. Phys. Comm.* **130** (2000) 260
7. PHYTHIA version 5.772 and JETSET version 7.4; T. Sjöstrand, Preprint CERN-TH/7112/93 (1993), revised 1995; T. Sjöstrand, *Comp. Phys. Comm.* **82** (1994) 74
8. KORALW version 1.33; M. Skrzypek *et al.*, *Comp. Phys. Comm.* **94** (1996) 216; M. Skrzypek *et al.*, *Phys. Lett.* **B 372** (1996) 289
9. F.A. Berends, R. Pittau and R. Kleiss, *Comp. Phys. Comm.* **85** (1995) 437
10. PHOJET version 1.05; R. Engel, *Z. Phys.* **C66** (1995) 203; R. Engel, J. Ranft and S. Roesler, *Phys. Rev.* **D52** (1995) 1459
11. F.A. Berends, P.H. Daverfeldt and R. Kleiss, *Nucl. Phys.* **B 253** (1985) 441
12. The L3 detector simulation is based on GEANT 3.21, see R. Brun *et al.*, CERN report CERN DD/EE/84-1 (1984), revised 1987, and uses GHEISHA to simulate hadronic interactions, see H. Fesefeldt, RWTH Aachen report PITHA 85/02 (1985).